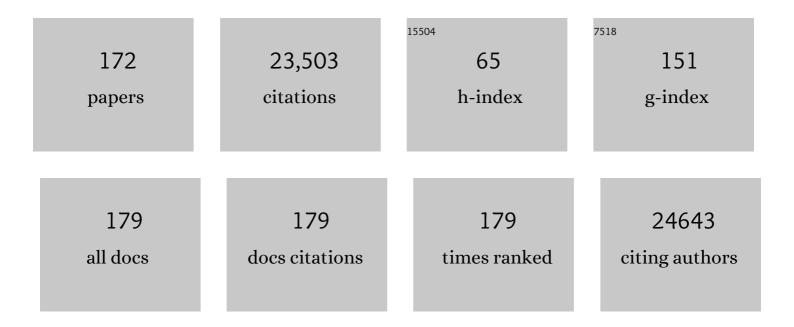
Haimei Zheng

List of Publications by Year in descending order

Source: https://exaly.com/author-pdf/9006714/publications.pdf Version: 2024-02-01



| # | Article | IF | CITATIONS |
|----|--|------|-----------|
| 1 | Epitaxial BiFeO3 Multiferroic Thin Film Heterostructures. Science, 2003, 299, 1719-1722. | 12.6 | 5,548 |
| 2 | Multiferroic BaTiO3-CoFe2O4 Nanostructures. Science, 2004, 303, 661-663. | 12.6 | 2,051 |
| 3 | Graphene Oxide as a Sulfur Immobilizer in High Performance Lithium/Sulfur Cells. Journal of the American Chemical Society, 2011, 133, 18522-18525. | 13.7 | 1,415 |
| 4 | Observation of Single Colloidal Platinum Nanocrystal Growth Trajectories. Science, 2009, 324, 1309-1312. | 12.6 | 1,200 |
| 5 | Real-Time Imaging of Pt ₃ Fe Nanorod Growth in Solution. Science, 2012, 336, 1011-1014. | 12.6 | 649 |
| 6 | Strain engineering and one-dimensional organization of metal–insulator domains in single-crystal vanadium dioxide beams. Nature Nanotechnology, 2009, 4, 732-737. | 31.5 | 562 |
| 7 | Highly porous non-precious bimetallic electrocatalysts for efficient hydrogen evolution. Nature Communications, 2015, 6, 6567. | 12.8 | 440 |
| 8 | Photovoltaic Devices Employing Ternary PbS _{<i>x</i>} Se _{1<i>-x</i>} Nanocrystals. Nano Letters, 2009, 9, 1699-1703. | 9.1 | 433 |
| 9 | Facet development during platinum nanocube growth. Science, 2014, 345, 916-919. | 12.6 | 429 |
| 10 | Electric Field-Induced Magnetization Switching in Epitaxial Columnar Nanostructures. Nano Letters, 2005, 5, 1793-1796. | 9.1 | 426 |
| 11 | Selective Facet Reactivity during Cation Exchange in Cadmium Sulfide Nanorods. Journal of the American Chemical Society, 2009, 131, 5285-5293. | 13.7 | 372 |
| 12 | Co-occurrence of Superparamagnetism and Anomalous Hall Effect in Highly Reduced Cobalt-Doped RutileTiO2â^îfFilms. Physical Review Letters, 2004, 92, 166601. | 7.8 | 352 |
| 13 | Synthesis of PbS Nanorods and Other Ionic Nanocrystals of Complex Morphology by Sequential Cation Exchange Reactions. Journal of the American Chemical Society, 2009, 131, 16851-16857. | 13.7 | 329 |
| 14 | Self-Assembled Growth of BiFeO3–CoFe2O4 Nanostructures. Advanced Materials, 2006, 18, 2747-2752. | 21.0 | 317 |
| 15 | Visualization of Electrode–Electrolyte Interfaces in LiPF ₆ /EC/DEC Electrolyte for Lithium Ion Batteries via in Situ TEM. Nano Letters, 2014, 14, 1745-1750. | 9.1 | 304 |
| 16 | Nanocrystal Diffusion in a Liquid Thin Film Observed by in Situ Transmission Electron Microscopy. Nano Letters, 2009, 9, 2460-2465. | 9.1 | 282 |
| 17 | Electrically Assisted Magnetic Recording in Multiferroic Nanostructures. Nano Letters, 2007, 7, 1586-1590. | 9.1 | 268 |
| 18 | Controlling Self-Assembled Perovskiteâ^'Spinel Nanostructures. Nano Letters, 2006, 6, 1401-1407. | 9.1 | 256 |

| # | Article | IF | CITATIONS |
|----|---|------|-----------|
| 19 | Epitaxial BiFeO3 thin films on Si. Applied Physics Letters, 2004, 85, 2574-2576. | 3.3 | 249 |
| 20 | Hetero-Epitaxial Anion Exchange Yields Single-Crystalline Hollow Nanoparticles. Journal of the American Chemical Society, 2009, 131, 13943-13945. | 13.7 | 221 |
| 21 | Observation of Transient Structural-Transformation Dynamics in a Cu ₂ S Nanorod. Science, 2011, 333, 206-209. | 12.6 | 220 |
| 22 | Nitrogen-doped cobalt phosphate@nanocarbon hybrids for efficient electrocatalytic oxygen reduction. Energy and Environmental Science, 2016, 9, 2563-2570. | 30.8 | 216 |
| 23 | Surfaceâ€Confined Fabrication of Ultrathin Nickel Cobaltâ€Layered Double Hydroxide Nanosheets for Highâ€Performance Supercapacitors. Advanced Functional Materials, 2018, 28, 1803272. | 14.9 | 215 |
| 24 | Ferroelectric size effects in multiferroic BiFeO3 thin films. Applied Physics Letters, 2007, 90, 252906. | 3.3 | 180 |
| 25 | A spongy nickel-organic CO ₂ reduction photocatalyst for nearly 100% selective CO production. Science Advances, 2017, 3, e1700921. | 10.3 | 175 |
| 26 | In-situ liquid cell transmission electron microscopy investigation on oriented attachment of gold nanoparticles. Nature Communications, 2018, 9, 421. | 12.8 | 171 |
| 27 | Formation of two-dimensional transition metal oxide nanosheets with nanoparticles as intermediates. Nature Materials, 2019, 18, 970-976. | 27.5 | 169 |
| 28 | Self-assembled single-crystal ferromagnetic iron nanowires formed by decomposition. Nature Materials, 2004, 3, 533-538. | 27.5 | 165 |
| 29 | Revealing the Atomic Restructuring of Pt–Co Nanoparticles. Nano Letters, 2014, 14, 3203-3207. | 9.1 | 162 |
| 30 | Revealing Bismuth Oxide Hollow Nanoparticle Formation by the Kirkendall Effect. Nano Letters, 2013, 13, 5715-5719. | 9.1 | 157 |
| 31 | Direct Observation of Nanoparticle Superlattice Formation by Using Liquid Cell Transmission Electron Microscopy. ACS Nano, 2012, 6, 2078-2085. | 14.6 | 152 |
| 32 | Determination of the Quantum Dot Band Gap Dependence on Particle Size from Optical Absorbance and Transmission Electron Microscopy Measurements. ACS Nano, 2012, 6, 9021-9032. | 14.6 | 138 |
| 33 | In Situ Study of Lithiation and Delithiation of MoS ₂ Nanosheets Using Electrochemical Liquid Cell Transmission Electron Microscopy. Nano Letters, 2015, 15, 5214-5220. | 9.1 | 135 |
| 34 | Three-dimensional heteroepitaxy in self-assembled BaTiO3–CoFe2O4 nanostructures. Applied Physics Letters, 2004, 85, 2035-2037. | 3.3 | 132 |
| 35 | Towards data-driven next-generation transmission electron microscopy. Nature Materials, 2021, 20, 274-279. | 27.5 | 130 |
| 36 | Observation of growth of metal nanoparticles. Chemical Communications, 2013, 49, 11720. | 4.1 | 128 |

| # | Article | IF | CITATIONS |
|----|---|------|-----------|
| 37 | Preparation of Singleâ€Layer MoS ₂ <i>_x</i> Se _{2(1â€} <i>_x</i> _x Mo <i>_x</i> S _x Mo <i>_x</i> Mo <i>_x</i> S _x Mo <i>_x</i> | 10.0 | 126 |
| 38 | Dynamic Covalent Synthesis of Crystalline Porous Graphitic Frameworks. CheM, 2020, 6, 933-944. | 11.7 | 123 |
| 39 | Structure and interface chemistry of perovskite-spinel nanocomposite thin films. Applied Physics Letters, 2006, 89, 172902. | 3.3 | 122 |
| 40 | Liquid Cell Transmission Electron Microscopy. Annual Review of Physical Chemistry, 2016, 67, 719-747. | 10.8 | 120 |
| 41 | Liquid Cell Transmission Electron Microscopy Study of Platinum Iron Nanocrystal Growth and Shape Evolution. Journal of the American Chemical Society, 2013, 135, 5038-5043. | 13.7 | 117 |
| 42 | In Situ Observation of Oscillatory Growth of Bismuth Nanoparticles. Nano Letters, 2012, 12, 1470-1474. | 9.1 | 114 |
| 43 | Sulfidation of Cadmium at the Nanoscale. ACS Nano, 2008, 2, 1452-1458. | 14.6 | 113 |
| 44 | Size effects in ultrathin epitaxial ferroelectric heterostructures. Applied Physics Letters, 2004, 84, 5225-5227. | 3.3 | 112 |
| 45 | Evidence for power-law frequency dependence of intrinsic dielectric response in theCaCu3Ti4O12. Physical Review B, 2004, 70, . | 3.2 | 110 |
| 46 | Assembled Monolayer Nanorod Heterojunctions. ACS Nano, 2011, 5, 3811-3816. | 14.6 | 109 |
| 47 | Frontiers of <i>in situ</i> electron microscopy. MRS Bulletin, 2015, 40, 12-18. | 3.5 | 109 |
| 48 | Imaging Protein Structure in Water at 2.7Ânm Resolution by Transmission Electron Microscopy. Biophysical Journal, 2012, 102, L15-L17. | 0.5 | 105 |
| 49 | CO2 Hydrogenation Studies on Co and CoPt Bimetallic Nanoparticles Under Reaction Conditions Using TEM, XPS and NEXAFS. Topics in Catalysis, 2011, 54, 778-785. | 2.8 | 103 |
| 50 | An investigation of ultrathin nickel-iron layered double hydroxide nanosheets grown on nickel foam for high-performance supercapacitor electrodes. Journal of Alloys and Compounds, 2017, 714, 63-70. | 5.5 | 101 |
| 51 | Electric Field Effect in Diluted Magnetic Insulator AnataseCo:  TiO2. Physical Review Letters, 2005, 94, 126601. | 7.8 | 100 |
| 52 | Direct observation of stick-slip movements of water nanodroplets induced by an electron beam. Proceedings of the National Academy of Sciences of the United States of America, 2012, 109, 7187-7190. | 7.1 | 97 |
| 53 | Heterophase fcc-2H-fcc gold nanorods. Nature Communications, 2020, 11, 3293. | 12.8 | 92 |
| 54 | One-pot synthesis of carbon coated-SnO2/graphene-sheet nanocomposite with highly reversible lithium storage capability. Journal of Power Sources, 2013, 232, 152-158. | 7.8 | 91 |

| # | Article | IF | CITATIONS |
|----|---|------|-----------|
| 55 | Nickel sulfide nanostructures prepared by laser irradiation for efficient electrocatalytic hydrogen evolution reaction and supercapacitors. Chemical Engineering Journal, 2019, 367, 115-122. | 12.7 | 90 |
| 56 | Heteroepitaxially enhanced magnetic anisotropy in BaTiO3–CoFe2O4 nanostructures. Applied Physics Letters, 2007, 90, 113113. | 3.3 | 88 |
| 57 | Size-Dependent Polar Ordering in Colloidal GeTe Nanocrystals. Nano Letters, 2011, 11, 1147-1152. | 9.1 | 84 |
| 58 | Revealing Correlation of Valence State with Nanoporous Structure in Cobalt Catalyst Nanoparticles by <i>In Situ</i> Environmental TEM. ACS Nano, 2012, 6, 4241-4247. | 14.6 | 84 |
| 59 | Structural and Morphological Evolution of Lead Dendrites during Electrochemical Migration. Scientific Reports, 2013, 3, 3227. | 3.3 | 83 |
| 60 | Tracking Nanoparticle Diffusion and Interaction during Self-Assembly in a Liquid Cell. Nano Letters, 2017, 17, 15-20. | 9.1 | 82 |
| 61 | Electron Beam Manipulation of Nanoparticles. Nano Letters, 2012, 12, 5644-5648. | 9.1 | 80 |
| 62 | SnS2 nanoparticle loaded graphene nanocomposites for superior energy storage. Physical Chemistry Chemical Physics, 2012, 14, 6981. | 2.8 | 79 |
| 63 | Thermoelectric Effect across the Metalâ^'Insulator Domain Walls in VO ₂ Microbeams. Nano Letters, 2009, 9, 4001-4006. | 9.1 | 77 |
| 64 | <i>In Situ</i> TEM Study of Catalytic Nanoparticle Reactions in Atmospheric Pressure Gas Environment. Microscopy and Microanalysis, 2013, 19, 1558-1568. | 0.4 | 72 |
| 65 | High-performance carbon nanotube transistors on SrTiO3/Si substrates. Applied Physics Letters, 2004, 84, 1946-1948. | 3.3 | 70 |
| 66 | Nanocomposites from Solution‣ynthesized PbTeâ€BiSbTe Nanoheterostructure with Unity Figure of Merit at Lowâ€Medium Temperatures (500–600 K). Advanced Materials, 2017, 29, 1605140. | 21.0 | 70 |
| 67 | In situ TEM study of the Li–Au reaction in an electrochemical liquid cell. Faraday Discussions, 2014, 176, 95-107. | 3.2 | 60 |
| 68 | Visualization of the Coalescence of Bismuth Nanoparticles. Microscopy and Microanalysis, 2014, 20, 416-424. | 0.4 | 58 |
| 69 | Electrode roughness dependent electrodeposition of sodium at the nanoscale. Nano Energy, 2020, 72, 104721. | 16.0 | 54 |
| 70 | Dynamic deformability of individual PbSe nanocrystals during superlattice phase transitions. Science Advances, 2019, 5, eaaw5623. | 10.3 | 52 |
| 71 | In Situ Study of Fe ₃ Pt–Fe ₂ O ₃ Core–Shell Nanoparticle Formation. Journal of the American Chemical Society, 2015, 137, 14850-14853. | 13.7 | 51 |
| 72 | Controlled Synthesis and Size-Dependent Polarization Domain Structure of Colloidal Germanium Telluride Nanocrystals. Journal of the American Chemical Society, 2011, 133, 2044-2047. | 13.7 | 49 |

| # | Article | IF | CITATIONS |
|----|--|------|-----------|
| 73 | Nanostructured flexible Mg-modified LiMnPO ₄ matrix as high-rate cathode materials for Li-ion batteries. Journal of Materials Chemistry A, 2014, 2, 6368-6373. | 10.3 | 47 |
| 74 | Highly efficient and wellâ€controlled ambient temperature RAFT polymerization of glycidyl methacrylate under visible light radiation. Journal of Polymer Science Part A, 2007, 45, 5091-5102. | 2.3 | 45 |
| 75 | MoS ₂ Liquid Cell Electron Microscopy Through Clean and Fast Polymer-Free MoS ₂ Transfer. Nano Letters, 2019, 19, 1788-1795. | 9.1 | 45 |
| 76 | Unveiling the mechanisms of lithium dendrite suppression by cationic polymer film induced solid–electrolyte interphase modification. Energy and Environmental Science, 2020, 13, 1832-1842. | 30.8 | 45 |
| 77 | Visualization of facet-dependent pseudo-photocatalytic behavior of TiO2 nanorods for water splitting using In situ liquid cell TEM. Nano Energy, 2019, 62, 507-512. | 16.0 | 44 |
| 78 | Selective Placement of Faceted Metal Tips on Semiconductor Nanorods. Angewandte Chemie - International Edition, 2013, 52, 980-982. | 13.8 | 43 |
| 79 | Tuning Complex Transition Metal Hydroxide Nanostructures as Active Catalysts for Water Oxidation by a Laser–Chemical Route. Nano Letters, 2015, 15, 2498-2503. | 9.1 | 42 |
| 80 | Crystallization of Mordenite Platelets using Cooperative Organic Structure-Directing Agents. Journal of the American Chemical Society, 2019, 141, 20155-20165. | 13.7 | 42 |
| 81 | Chemically Stable Polyarylether-Based Metallophthalocyanine Frameworks with High Carrier Mobilities for Capacitive Energy Storage. Journal of the American Chemical Society, 2021, 143, 17701-17707. | 13.7 | 42 |
| 82 | Visualization of Colloidal Nanocrystal Formation and Electrode–Electrolyte Interfaces in Liquids Using TEM. Accounts of Chemical Research, 2017, 50, 1808-1817. | 15.6 | 40 |
| 83 | In Situ Study of Spinel Ferrite Nanocrystal Growth Using Liquid Cell Transmission Electron Microscopy. Chemistry of Materials, 2015, 27, 8146-8152. | 6.7 | 39 |
| 84 | Dynamics of Nanoscale Dendrite Formation in Solution Growth Revealed Through in Situ Liquid Cell Electron Microscopy. Nano Letters, 2018, 18, 6427-6433. | 9.1 | 38 |
| 85 | Modification of critical current density of MgB2 films irradiated with 200 MeV Ag ions. Applied Physics Letters, 2004, 84, 2352-2354. | 3.3 | 37 |
| 86 | Partial Dislocations in Graphene and Their Atomic Level Migration Dynamics. Nano Letters, 2015, 15, 5950-5955. | 9.1 | 37 |
| 87 | Tracking the Effects of Ligands on Oxidative Etching of Gold Nanorods in Graphene Liquid Cell Electron Microscopy. ACS Nano, 2020, 14, 10239-10250. | 14.6 | 35 |
| 88 | Dynamic behavior of nanoscale liquids in graphene liquid cells revealed by in situ transmission electron microscopy. Micron, 2019, 116, 22-29. | 2.2 | 31 |
| 89 | Self-assembled vertical heteroepitaxial nanostructures: from growth to functionalities. MRS Communications, 2014, 4, 31-44. | 1.8 | 29 |
| 90 | Electrically driven cation exchange for in situ fabrication of individual nanostructures. Nature Communications, 2017, 8, 14889. | 12.8 | 29 |

| # | Article | IF | CITATIONS |
|-----|---|------|-----------|
| 91 | Selective nitrogen doping of graphene oxide by laser irradiation for enhanced hydrogen evolution activity. Chemical Communications, 2018, 54, 13726-13729. | 4.1 | 28 |
| 92 | In situ TEM observation of calcium silicate hydrate nanostructure at high temperatures. Cement and Concrete Research, 2021, 149, 106579. | 11.0 | 28 |
| 93 | Perspectives on in situ electron microscopy. Ultramicroscopy, 2017, 180, 188-196. | 1.9 | 26 |
| 94 | Liquid phase transmission electron microscopy for imaging of nanoscale processes in solution. MRS Bulletin, 2020, 45, 704-712. | 3.5 | 26 |
| 95 | On-Column 2 <i>p</i> Bound State with Topological Charge ±1 Excited by an Atomic-Size Vortex Beam in an Aberration-Corrected Scanning Transmission Electron Microscope. Microscopy and Microanalysis, 2012, 18, 711-719. | 0.4 | 24 |
| 96 | Using molecular tweezers to move and image nanoparticles. Nanoscale, 2013, 5, 4070. | 5.6 | 24 |
| 97 | Selfâ€Passivation of Defects: Effects of Highâ€Energy Particle Irradiation on the Elastic Modulus of Multilayer Graphene. Advanced Materials, 2015, 27, 6841-6847. | 21.0 | 24 |
| 98 | Aggregation dynamics of nanoparticles at solid–liquid interfaces. Nanoscale, 2017, 9, 10044-10050. | 5.6 | 24 |
| 99 | Nanoscale x-ray magnetic circular dichroism probing of electric-field-induced magnetic switching in multiferroic nanostructures. Applied Physics Letters, 2007, 90, 123104. | 3.3 | 23 |
| 100 | Revealing of the Activation Pathway and Cathode Electrolyte Interphase Evolution of Li-Rich 0.5Li ₂ MnO ₃ ·0.5LiNi _{0.3} Co _{0.3} Mn _{0.4} O _{2< Cathode by in Situ Electrochemical Quartz Crystal Microbalance. ACS Applied Materials & amp; Interfaces, 2019, 11, 16214-16222.} | | 23 |
| 101 | Strain-Mediated Interfacial Dynamics during Au–PbS Core–Shell Nanostructure Formation. ACS Nano, 2016, 10, 6235-6240. | 14.6 | 21 |
| 102 | Identifying surface structural changes in a newly-developed Ga-based alloy with melting temperature below 10â€Â°C. Applied Surface Science, 2019, 492, 143-149. | 6.1 | 21 |
| 103 | Structural and Chemical Evolution of Amorphous Nickel Iron Complex Hydroxide upon Lithiation/Delithiation. Chemistry of Materials, 2015, 27, 1583-1589. | 6.7 | 20 |
| 104 | In-situ Multimodal Imaging and Spectroscopy of Mg Electrodeposition at Electrode-Electrolyte Interfaces. Scientific Reports, 2017, 7, 42527. | 3.3 | 20 |
| 105 | In situ TEM observation of neck formation during oriented attachment of PbSe nanocrystals. Nano Research, 2019, 12, 2549-2553. | 10.4 | 20 |
| 106 | Epitaxially induced high temperature (>900K) cubic-tetragonal structural phase transition in BaTiO3 thin films. Applied Physics Letters, 2004, 85, 4109-4111. | 3.3 | 19 |
| 107 | Bubble nucleation and migration in a lead–iron hydr(oxide) core–shell nanoparticle. Proceedings of the United States of America, 2015, 112, 12928-12932. | 7.1 | 19 |
| 108 | Revealing Cation-Exchange-Induced Phase Transformations in Multielemental Chalcogenide Nanoparticles. Chemistry of Materials, 2017, 29, 9192-9199. | 6.7 | 19 |

| # | Article | IF | CITATIONS |
|-----|--|------|-----------|
| 109 | Solid–liquid–gas reaction accelerated by gas molecule tunnelling-like effect. Nature Materials, 2022, 21, 859-863. | 27.5 | 19 |
| 110 | In Situ TEM Study of the Degradation of PbSe Nanocrystals in Air. Chemistry of Materials, 2019, 31, 190-199. | 6.7 | 18 |
| 111 | Defect-mediated ripening of core-shell nanostructures. Nature Communications, 2022, 13, 2211. | 12.8 | 17 |
| 112 | Origin of antiphase domain boundaries and their effect on the dielectric constant of Ba0.5Sr0.5TiO3 films grown on MgO substrates. Applied Physics Letters, 2002, 81, 4398-4400. | 3.3 | 16 |
| 113 | Electrical Breakdown of Suspended Mono- and Few-Layer Tungsten Disulfide <i>via</i> Sulfur Depletion Identified by <i>in Situ</i> Atomic Imaging. ACS Nano, 2017, 11, 9435-9444. | 14.6 | 16 |
| 114 | Understanding the role of water-soluble guar gum binder in reducing capacity fading and voltage decay of Li-rich cathode for Li-ion batteries. Electrochimica Acta, 2020, 351, 136401. | 5.2 | 16 |
| 115 | Growth mechanism of core–shell PtNi–Ni nanoparticles using in situ transmission electron microscopy. Nanoscale, 2018, 10, 11281-11286. | 5.6 | 15 |
| 116 | Identification of a quasi-liquid phase at solid–liquid interface. Nature Communications, 2022, 13, . | 12.8 | 15 |
| 117 | Size and shape evolution of embedded single-crystal α-Fe nanowires. Applied Physics Letters, 2005, 87, 203110. | 3.3 | 14 |
| 118 | Suppression of antiphase domain boundary formation in Ba0.5Sr0.5TiO3 films grown on vicinal MgO substrates. Applied Physics Letters, 2004, 85, 2905-2907. | 3.3 | 13 |
| 119 | Facile synthesis of wellâ€defined pHâ€liable Schiffâ€baseâ€type photosensitive polymers via visibleâ€lightâ€activated ambient temperature RAFT polymerization. Journal of Polymer Science Part A, 2009, 47, 6668-6681. | 2.3 | 13 |
| 120 | Controlling electron beam-induced structure modifications and cation exchange in cadmium sulfide–copper sulfide heterostructured nanorods. Ultramicroscopy, 2013, 134, 207-213. | 1.9 | 13 |
| 121 | Imaging, understanding, and control of nanoscale materials transformations. MRS Bulletin, 2021, 46, 443-450. | 3.5 | 13 |
| 122 | Tailoring Transitionâ€Metal Hydroxides and Oxides by Photonâ€Induced Reactions. Angewandte Chemie - International Edition, 2016, 55, 14272-14276. | 13.8 | 11 |
| 123 | Spring-Like Pseudoelectroelasticity of Monocrystalline Cu ₂ S Nanowire. Nano Letters, 2018, 18, 5070-5077. | 9.1 | 11 |
| 124 | Negative Electro-conductance in Suspended 2D WS ₂ Nanoscale Devices. ACS Applied Materials & Interfaces, 2016, 8, 32963-32970. | 8.0 | 10 |
| 125 | Growth and assembly of cobalt oxide nanoparticle rings at liquid nanodroplets with solid junction. Nanoscale, 2017, 9, 13915-13921. | 5.6 | 10 |
| 126 | Spontaneous Reshaping and Splitting of AgCl Nanocrystals under Electron Beam Illumination. Small, 2018, 14, e1803231. | 10.0 | 10 |

| # | Article | IF | CITATIONS |
|-----|--|------|-----------|
| 127 | Observation of Surface Ligands-Controlled Etching of Palladium Nanocrystals. Nano Letters, 2021, 21, 6640-6647. | 9.1 | 10 |
| 128 | Transmission Electron Microscopy for Chemists. Accounts of Chemical Research, 2017, 50, 1795-1796. | 15.6 | 9 |
| 129 | Efficient CO2 reduction MOFs derivatives transformation mechanism revealed by in-situ liquid phase TEM. Applied Catalysis B: Environmental, 2022, 307, 121164. | 20.2 | 9 |
| 130 | Real time imaging of two-dimensional iron oxide spherulite nanostructure formation. Nano Research, 2019, 12, 2889-2893. | 10.4 | 8 |
| 131 | Controlled oxidative etching of gold nanorods revealed through in-situ liquid cell electron microscopy. Science China Materials, 2020, 63, 2599-2605. | 6.3 | 8 |
| 132 | Local dielectric measurements of BaTiO3–CoFe2O4 nanocomposites through microwave microscopy. Journal of Materials Research, 2007, 22, 1193-1199. | 2.6 | 7 |
| 133 | Revealing Dynamic Processes of Materials in Liquids Using Liquid Cell Transmission Electron Microscopy. Journal of Visualized Experiments, 2012, , . | 0.3 | 7 |
| 134 | Scanning Confocal Electron Energy-Loss Microscopy Using Valence-Loss Signals. Microscopy and Microanalysis, 2013, 19, 1036-1049. | 0.4 | 7 |
| 135 | A unique pathway of PtNi nanoparticle formation observed with liquid cell transmission electron microscopy. Nanoscale, 2020, 12, 1414-1418. | 5.6 | 7 |
| 136 | Recent progress in thermoelectric nanocomposites based on solution-synthesized nanoheterostructures. Nano Research, 2017, 10, 1498-1509. | 10.4 | 6 |
| 137 | Anomalously high electronic thermal conductivity and Lorenz ratio in Bi2Te3 nanoribbons far from the bipolar condition. Applied Physics Letters, 2019, 114, . | 3.3 | 5 |
| 138 | Dynamics of Polymer Nanocapsule Buckling and Collapse Revealed by <i>In Situ</i> Liquid-Phase TEM. Langmuir, 2022, 38, 7168-7178. | 3.5 | 5 |
| 139 | Hybrid nanocapsules for <i>in situ</i> TEM imaging of gas evolution reactions in confined liquids. Nanoscale, 2020, 12, 18606-18615. | 5.6 | 4 |
| 140 | Efficient Enhancement of Stability and Luminescence of Three-Dimensional CsPbBr ₃ Nanoparticles via Ligand-Triggered Transformation into Zero-Dimensional Cs ₄ PbBr ₆ Nanoparticles. Journal of Physical Chemistry C, 2022, 126, 4172-4181. | 3.1 | 4 |
| 141 | Real time observation of gold nanoparticle aggregation dynamics on a 2D membrane. Microscopy and Microanalysis, 2016, 22, 808-809. | 0.4 | 3 |
| 142 | Liquid Pockets Encapsulated in MoS2 Liquid Cells. Microscopy and Microanalysis, 2019, 25, 1406-1407. | 0.4 | 3 |
| 143 | Influence of sub-zero temperature on nucleation and growth of copper nanoparticles in electrochemical reactions. IScience, 2021, 24, 103289. | 4.1 | 3 |
| 144 | Imaging of Pt3Fe Nanwire Growth in Liquids by In situ TEM. Microscopy and Microanalysis, 2012, 18, 1092-1093. | 0.4 | 2 |

| # | Article | IF | CITATIONS |
|-----|---|-----|-----------|
| 145 | Growth of Transition Metal Oxides in Solution under Liquid Cell Electron Microscopy and Electron Beam Effects. Microscopy and Microanalysis, 2015, 21, 1123-1124. | 0.4 | 2 |
| 146 | Tailoring Transitionâ€Metal Hydroxides and Oxides by Photonâ€Induced Reactions. Angewandte Chemie, 2016, 128, 14484-14488. | 2.0 | 2 |
| 147 | Anomalous Shape Evolution of Ag ₂ O ₂ Nanocrystals Modulated by Surface Adsorbates during Electron Beam Etching. Nano Letters, 2019, 19, 591-597. | 9.1 | 2 |
| 148 | Generating and Capturing Secondary Hot Carriers in Monolayer Tungsten Dichalcogenides. Journal of Physical Chemistry Letters, 2022, 13, 5703-5710. | 4.6 | 2 |
| 149 | Quantitative Confocal Sectioning in Double-Corrected STEM Utilizing Electron Energy Loss Spectroscopy and Post-Specimen Cc Correction. Microscopy and Microanalysis, 2012, 18, 1026-1027. | 0.4 | 1 |
| 150 | Response to "Electron Microscopy of Biological Specimens in Liquid Water― Biophysical Journal, 2012, 103, 165-166. | 0.5 | 1 |
| 151 | Imaging Protein in Water with Nanometer Resolution. Biophysical Journal, 2012, 102, 386a-387a. | 0.5 | 1 |
| 152 | Electrochemical conversion and storage systems: general discussion. Faraday Discussions, 2014, 176, 153-184. | 3.2 | 1 |
| 153 | Nanostructure Growth, Interactions, and Assembly in the Liquid Phase. , 0, , 191-209. | | 1 |
| 154 | Insights into the Defect Structure Resulting from the Hydrogen Absorption in Palladium Nanocubes Using Liquid Cell Transmission Electron Microscopy. Microscopy and Microanalysis, 2021, 27, 2100-2101. | 0.4 | 1 |
| 155 | Magneto-Optical Kerr Effect in Multiferroic Nanostructures. Materials Research Society Symposia Proceedings, 2006, 966, 1. | 0.1 | 0 |
| 156 | Observation of Dynamic Structural Transformations in a Copper Sulfide Nanorod by TEM. Microscopy and Microanalysis, 2011, 17, 1644-1645. | 0.4 | 0 |
| 157 | Nanometer-Scale Electron Microscopy of Proteins in Liquid. Microscopy and Microanalysis, 2011, 17, 120-121. | 0.4 | Ο |
| 158 | Observation of Single Nanocrystal Growth Trajectories in Solution Using Liquid Cell TEM. Microscopy and Microanalysis, 2011, 17, 1716-1717. | 0.4 | 0 |
| 159 | Revealing Correlation of Valence State with Structural Coarsening in Nanoporous Co/Silica Catalysts by in situ Environmental TEM and EELS. Microscopy and Microanalysis, 2012, 18, 1116-1117. | 0.4 | Ο |
| 160 | Transmission Electron Microscopy Imaging of Structural Transformation Dynamics in a Single Nanocrystal. Microscopy Today, 2012, 20, 18-22. | 0.3 | 0 |
| 161 | In-situ Electrochemical Liquid Cell TEM Visualization of Electrode-Electrolyte Interfaces. Microscopy and Microanalysis, 2014, 20, 424-425. | 0.4 | 0 |
| 162 | The Two Dimensional Nanoplate Dynamics Revealed by in situ Liquid Cell TEM. Microscopy and Microanalysis, 2015, 21, 261-262. | 0.4 | 0 |

| # | Article | IF | CITATIONS |
|-----|--|------|-----------|
| 163 | Liquid Cell TEM Study of Nanoparticle Diffusion and Interaction in Liquids. Microscopy and Microanalysis, 2016, 22, 742-743. | 0.4 | 0 |
| 164 | Liquid Cell TEM Observation of Platinum Based Alloy Nanoparticle Growth. Microscopy and Microanalysis, 2017, 23, 1980-1981. | 0.4 | 0 |
| 165 | Visualization of Electrochemical Reaction Dynamics in Liquids Using TEM. Microscopy and Microanalysis, 2017, 23, 884-885. | 0.4 | 0 |
| 166 | Nanocrystal Dynamics: Spontaneous Reshaping and Splitting of AgCl Nanocrystals under Electron Beam Illumination (Small 48/2018). Small, 2018, 14, 1870231. | 10.0 | 0 |
| 167 | In-situ TEM Study on Sub-10 nm Materials. Microscopy and Microanalysis, 2018, 24, 1650-1651. | 0.4 | 0 |
| 168 | Liquid Cell TEM Study of Nucleation and Growth of Dendrites. Microscopy and Microanalysis, 2018, 24, 250-251. | 0.4 | 0 |
| 169 | Diffraction imaging of organic materials in extreme environments. Microscopy and Microanalysis, 2021, 27, 1802-1803. | 0.4 | 0 |
| 170 | Development of liquid cells for high resolution imaging and chemical analysis in situ with Transmission Electron Microscopy. Microscopy and Microanalysis, 2021, 27, 804-806. | 0.4 | 0 |
| 171 | Radiolysis Characterization in Liquid Cell STEM Using Ultra Low-Dose Electron Energy-Loss Spectroscopy. Microscopy and Microanalysis, 2021, 27, 2626-2628. | 0.4 | 0 |
| 172 | SnS2-Graphene Nanocomposite for Advanced Lithium-Ion Battery. ECS Meeting Abstracts, 2012, , . | 0.0 | 0 |